Materials Science and Engineering A 507 (2009) 236–240

Contents lists available at ScienceDirect

Materials Science and Engineering A

journal homepage: www.elsevier.com/locate/msea

On the uniform elongation of cast Al–7%Si–0.6%Mg (A357) alloys

Nikolaos D. Alexopoulos [a], Murat Tiryakioğlu [b,*]

[a] University of the Aegean, Department of Financial and Management Engineering, 821 00, Chios, Greece
[b] Department of Engineering, Robert Morris University, Moon Township, PA 15108, USA

A R T I C L E I N F O

Article history:
Received 17 September 2008
Received in revised form 3 December 2008
Accepted 3 December 2008

Keywords:
Strain-hardening exponent
Kocks–Mecking
Nonuniform elongation
Structural defects

A B S T R A C T

Continuously cast A357 alloy specimens that are essentially free from structural defects, such as oxide bifilms and porosity, were artificially aged at three different temperatures for various durations. The stress–strain curves of 90 specimens were analyzed. It was determined that in A357: (i) nonuniform elongation can be up to 38% of total elongation, (ii) nonuniform elongation can be as high as 5%, (iii) for the same yield strength, uniform elongation is a lower fraction of the total elongation in the overaged specimens than in the underaged, (iv) the strain-hardening exponent, n, of the Ludwik–Hollomon equation changes linearly with yield strength in underaged and overaged conditions, (v) n provides a poor estimate of the uniform elongation, and (vi) the Voce equation estimates the uniform elongation accurately.

© 2008 Elsevier B.V. All rights reserved.

1. Introduction

Aluminum–silicon casting alloys offer a good combination of mechanical properties and castability, which accounts for their wide use in automotive and aerospace applications. Nevertheless aluminum castings have been rarely used in critical applications due to concerns about the variability in properties, especially in elongation and fatigue life. This high level of variability is a consequence of structural defects in castings, i.e., pores and oxide bifilms, which degrade mechanical properties; they cause premature fracture in tension [1] and fatigue [2], resulting in low ductility, tensile strength and fatigue life [3]. In addition, the presence of major structural defects result in increased variability in properties, as evidenced most notably by lower Weibull moduli [4,5]. Hence minimization and even elimination of the structural defects is vital for wider use of aluminum castings in structural applications in aerospace and automotive industry.

In the quest for improved properties it is helpful for the foundry engineer to have a metric to measure the degree of improvement that they make. The so-called quality indices developed over the years are intended to serve this need. Among the quality factors developed so far, only the ones by Cáceres [6] and Tiryakioğlu et al. [7] supply a measure in terms of the ratio of the current to achievable ductility. Both indices determine the achievable (or target) ductility from the work hardening characteristics of the specimen, assuming that there is no or negligible nonuniform elongation in specimens even when they are free from structural defects. To the authors' knowledge, nonuniform deformation in cast Al–7%Si–Mg alloys has not been investigated, mainly because the cast specimens typically have inherently high density of defects which cause premature failure in tension. In the present study, specimens were prepared by continuous casting so that they are essentially free from structural defects. The effect of artificial aging on uniform and nonuniform deformation in A357 casting alloys has been investigated and is reported in this paper. Moreover, the two constitutive equations used previously by Cáceres and Tiryakioğlu et al. are compared.

2. Background

The need to estimate potential, defect-free ductility of castings from tensile curves has become more apparent recently, during the efforts to develop new quality indices. Cáceres [6] developed a quality index, Q_C, which is a ratio of actual elongation, e_F, to elongation expected of the specimen if it were free from structural defects, $e_{F(e)}$:

$$Q_C = \frac{e_F}{e_{F(e)}} \tag{1}$$

Cáceres assumed that the true stress–true strain in cast aluminum alloys follows the well-known Ludwik–Hollomon equation:

$$\sigma = C\varepsilon_p^n \tag{2}$$

where σ and ε_p are true stress and true plastic strain, respectively, C is the strength coefficient and n is the strain-hardening exponent. In tension, uniform deformation takes place until the Considere

* Corresponding author.
E-mail address: tiryakioglu@rmu.edu (M. Tiryakioğlu).

0921-5093/$ – see front matter © 2008 Elsevier B.V. All rights reserved.
doi:10.1016/j.msea.2008.12.026

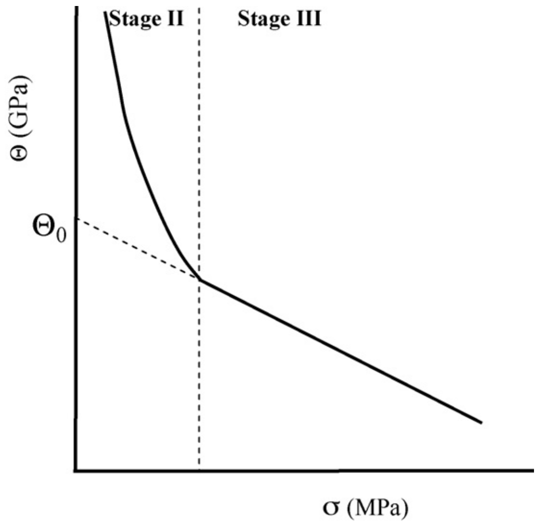

Fig. 1. Schematic illustration of the work hardening behavior observed in cast Al–Si–Mg alloys.

criterion is met, such that;

$$\frac{d\sigma}{d\varepsilon_p} = \sigma \quad (3)$$

Taking the derivative of Eq. (2) and inserting into Eq. (3), one can find that the Considere criterion is met when true uniform strain (ε_u) is equal to n [8]. In Al–7%Si–Mg alloy aerospace castings, McLellan [9] observed that fracture takes place without almost any necking. Hence, Cáceres assumed that fracture occurs at or before the nominal uniform elongation value, being approximated by as the uniform engineering strain $e_u \approx e_{F(e)} \approx n$.

Although the Ludwik–Hollomon equation has been used widely for the true stress–strain behavior of cast Al–7%Si–Mg alloys because of its simplicity, recent research [1,10–13] has shown that these alloys follow the Kocks–Mecking (KM) work hardening model, as shown schematically in Fig. 1. At high strain levels, work hardening follows Stage III, during which hardening and softening mechanisms compete. The relationship between work hardening rate and stress becomes linear in Stage III and is written as [14,15]:

$$\Theta = \frac{d\sigma}{d\varepsilon_p} = \Theta_0 - K\sigma \quad (4)$$

where Θ is the work hardening rate (MPa), σ is the true stress (MPa), ε_p is the true plastic strain, Θ_0 is the initial work hardening rate and K is a unitless parameter that is mainly dependent on Stage II work hardening rate, strain rate and includes the effect of precipitation hardening in heat-treatable alloys. Eq. (4), also referred to as the Kocks–Mecking work hardening model, has been widely used in the literature to study the work hardening characteristics of wrought aluminum alloys. Integrating Eq. (4) with respect to strain, we obtain the well-known Voce equation [16]:

$$\sigma = \sigma_\infty - (\sigma_\infty - \sigma_0)\exp(-K\varepsilon_p) \quad (5)$$

where σ_∞ is saturation stress (stress after which $\Theta = 0$) and σ_0 is stress at $\varepsilon = 0$. Combining Eqs. (3)–(5), the true uniform strain following the Kocks–Mecking model ($\varepsilon_{u|KM}$) can be found as

$$\varepsilon_{u|KM} = -\frac{1}{K}\ln\left(\frac{\sigma_\infty}{(K+1)(\sigma_\infty - \sigma_0)}\right) \quad (6)$$

In several studies, it was determined that structural defects in aluminum castings reduce the observed work hardening rates significantly [1,10,17]. Moreover, in specimens with major structural defects, a sudden drop in work hardening rate just before fracture was observed [1,10,17]. Consequently, Tiryakioğlu et al. [10] observed that that the late stages of work hardening (Stage III), where the Considere criterion is met, cannot be estimated accurately from earlier stages. Hence, if a specimen fractures prematurely due to the presence of structural defects, such as porosity and/or oxide bifilms, the extrapolation of work hardening characteristics to higher strains underestimates potential uniform and, of course, total elongation. Kocks and Mecking [18] stated that the Voce equation does not fit the entire stress–strain curve, but it provides a good fit in an extensive region, especially during the late stages of deformation, i.e., Stage III. The Ludwik–Hollomon equation, however, is fitted to the entire stress–strain curve, as outlined in the ASTM E646 standard. It is of interest to (i) generate uniform (and nonuniform) elongation data from specimens with essentially no structural defects, and (ii) compare the uniform elongation estimated by the two constitutive equations. This study fills this gap in the literature.

3. Experimental details

A357 alloy tensile specimens were excised from the center of continuously cast bars, courtesy of Pechiney (Vorrepe, France). The chemical composition of the delivered ingot material was Al–7.0Si–0.55Mg–0.10Ti–0.12Fe–<0.10Mn. The tensile specimens were machined according to the ASTM E8M specification with 5 mm thickness and 12.5 mm × 50 mm being the reduced cross section of the specimen. All specimens were solutions heat treated for 22 h at 540 °C and quenched in still water with ice at a temperature less than 10 °C, as proposed previously [19]. Subsequently, specimens were aged artificially at 155, 175 and 205 °C for various times without any aging delay. One specimen was tested in W temper. Tensile tests were conducted according to ASTM E8 at a constant deformation rate of $3.3 \times 10^{-4}\ s^{-1}$. True stress–true strain curves of the specimens were computed based on the conservation of volume in the uniform elongation regime. The work hardening rate at every stress data point was determined by a moving 11-point fitting scheme and its differentiation. A total of 90 tensile stress–strain curves were analyzed for the evaluation of the work hardening characteristics of the A357 castings. More details are provided in Refs. [20,21].

4. Results and discussion

4.1. Microstructure

Typical microstructures of the investigated cast aluminum alloy A357 are presented in Fig. 2. Note that Si particles are round and somewhat hexagonal. The secondary dendrite arm spacing (SDAS) was measured to be approximately 27 μm. The Si particle sizes, as measured in two-dimensions, were quantified by digital image analysis using ImagePro software. The average particle area and aspect ratio were found to be 7.31 μm^2 and 1.44, respectively. Statistical analysis showed [12] that both the area and aspect ratio of Si particles follow the lognormal distribution, which is in agreement with earlier studies [22–24]. More details on the characterization of microstructure are provided in Ref. [12].

4.2. Verification of structural quality

To ensure that the specimens are free from structural defects, fracture surfaces were investigated via scanning electron microscopy (SEM). A typical fractograph is presented in Fig. 3. Note that the fracture surface is dominated by dimples, implying that extensive deformation took place before final fracture. In addition, damaged Si particles were found in the analysis. Some damaged Si particles can be seen at the center of dimples, as indicated by arrows in Fig. 3.

Download English Version:

https://daneshyari.com/en/article/1581077

Download Persian Version:

https://daneshyari.com/article/1581077

Daneshyari.com